Thermodynamics of Dehydrogenation of the 2LiBH4-Mg2FeH6 Composite

Mohammad R Ghaani, Michele R Catti, Angeloclaudio R Nale

Thermodynamics of Dehydrogenation of the $2LiBH_4$-Mg_2FeH_6 Composite

Mohammad R. Ghaani, Michele Catti,* and Angeloclaudio Nale

Dipartimento di Scienza dei Materiali, Università di Milano Bicocca, via R. Cozzi 53, I-20125 Milano, Italy

ABSTRACT

Joint decomposition of hydrides may be energetically favored, if stable mixed compounds are formed. This 'hydride destabilization' improves the energetics of H_2 release from hydrogen storage materials. The sequence of dehydrogenation reactions of the $2LiBH_4$-Mg_2FeH_6 composite was studied by PCI (Pressure-Composition-Isotherm) and TPD (Temperature-Programmed-Desorption) techniques in a Sievert apparatus. Produced phases were identified by ex-situ X-ray diffraction and FTIR spectroscopy. Three distinct plateaus are detected on each isotherm: A, B, and C on decreasing pressure. The A reaction, involving formation of FeB, MgH_2 and LiH, occurs at higher pressure/lower temperature than dehydrogenation of either pure hydrides; these are then effectively destabilized thermodynamically. The B process is plain decomposition of MgH_2, and in C the magnesium produced reacts with $LiBH_4$ left forming MgB_2 and LiH. The B+C sequence is fully reversible, and it corresponds to two-step dehydrogenation of the $LiBH_4/MgH_2$ system. Reaction enthalpies and entropies were obtained through van't Hoff plots of all processes, thus providing a full thermodynamic characterization of the system.

Keywords: Hydride composite, hydrogen storage, dehydriding reaction, van't Hoff plot

1. INTRODUCTION

Within compounds of interest for hydrogen storage applications, metal hydrides and light metal borohydrides have been covered by extensive research work.[1-5] The first class of materials are characterized by moderate weight percent hydrogen yields, but they usually show good reversibility of the hydrogen exchange reaction. Borohydrides, on the other hand, have a quite large hydrogen content; however, in most cases their dehydrogenation is hardly reversible. Further, a common problem shared by both classes of hydrides is that they are thermodynamically more stable than desired, mainly because of their large decomposition enthalpies: they thus release hydrogen at rather high temperatures, raising a serious technological difficulty for applications. Such an issue was addressed by attempts to stabilize the dehydrogenation products of the hydride, in order to reduce the overall reaction enthalpy.[6] This may be achieved when different hydrides react together, if particularly stable mixed compounds are formed by dehydrogenation. Theoretical predictions confirm that this should be a promising way of improving the performances of hydrogen storage materials.[7]

This approach was applied in particular to $LiBH_4$, an important member of the borohydride family. Lithium borohydride is a well known system, with a high gravimetric H_2 density of 13.9 wt% (considering the LiH product as not decomposable), and with dehydrogenation occurring in the 400-600 °C thermal range at ambient pressure and without catalysts.[8] The reaction could be reversed only at high pressure and temperature.[9,10] Published work on $LiBH_4$ destabilizing dehydrogenation reactions concerns mainly the $LiBH_4$+MgH_2 system, which was investigated quite thoroughly.[10-13] Also systems involving two borohydrides, like the $LiBH_4$-$Mg(BH_4)_2$ assemblage, were considered in this respect.[14,15]

The present research deals with the reaction of hydrogen release from lithium borohydride associated with Mg_2FeH_6. This metal hydride was considered because of its good performance for hydrogen storage, and aiming at the possible formation of stable iron borides

which could favor the joint dehydrogenation process of both hydrides. Mg_2FeH_6 has an intermediate gravimetric (5.5 wt%) and a very high volumetric (150 kg m^{-3}) hydrogen density, thus proving to be a quite interesting material for hydrogen storage. Yet the synthesis of this metal hydride is not so simple to perform because no stable Mg-Fe binary compounds are available, so that either pure Mg and Fe or MgH_2 and Fe have to be employed as reagents, and some residual non-reacted Fe is often left with Mg_2FeH_6.[16-23]

The work was undertaken with the main goals of (i) characterizing the phase composition of dehydrogenation products of the $2LiBH_4$-Mg_2FeH_6 composite along the whole reaction step sequence, (ii) determining the *p(T)* phase boundaries of the different hydride assemblages, and (iii) deriving the thermodynamic parameters of the reactions involved. By comparison with the known behavior of the pure components $LiBH_4$ and Mg_2FeH_6, we expected possible energetic improvements due to formation of stable mixed compounds, so as to achieve lower *T*/higher *p* conditions for the dehydrogenation reaction.

2. EXPERIMENTAL

The Mg_2FeH_6 component was synthesized according to the route employing magnesium hydride and iron as reagents.[20,21] A 1.2 g sample of commercial MgH_2 and α-Fe (Sigma-Aldrich) in 2:1 molar ratio was loaded with ten 1 cm diameter stainless steel balls (ball-to-powder weight ratio = 30) into a vial of the same material. The powder was ball milled in Ar atmosphere by a Retsch planetary mill for 30 h at 400 rounds min^{-1}. Then the ball milled sample was loaded in an automatic Sievert-type apparatus (Advanced Materials Corporation), brought to $p(H_2)$ =100 bar and then heated at 400 °C for various times. Several reaction times were employed: 3, 4, 6, 9, and 14 days, in each case analyzing the final product by X-ray diffraction.

Samples of the $2LiBH_4$-Mg_2FeH_6 composite were prepared by mixing synthesized Mg_2FeH_6 powder with commercial $LiBH_4$ (Sigma-Aldrich) in a glove box filled with recirculated argon atmosphere. All subsequent handling of such samples took place in the glove box. Thermodynamic measurements of the hydrogenation/dehydrogenation reactions were done by the Sievert-type equipment. A 0.6 g sample of the composite was loaded into the 5 cm^3 reactor, located in a furnace with temperature control: after evacuation, hydrogen gas of high purity (99.9995%) was introduced at room temperature (RT) and high pressure (100 bar). Dehydrogenation experiments were performed in two different modes. Pressure-Composition-Isotherm (PCI) mode: the sample was heated to the target temperature, which was thereafter kept constant; then the pressure was progressively decreased from 100 to 0.1 bar by small steps of approximately 0.3 bar (desorption experiments). At each step, the sample was allowed to equilibrate until the rate of pressure change due to H_2 release was less than 1 mbar min^{-1}; in most cases, this condition was fulfilled within 2 h waiting time. Then the relative amount of hydrogen exchanged by the sample was computed by the system software. Temperature-programmed-desorption (TPD) dynamic mode: a temperature ramp from 25 to 550 °C with 1 °C min^{-1} rate, under H_2 high pressure (3 to 80 bar at RT), was set up; the pressure change due to bare heating was corrected using a calibration curve; the residual pressure increase was converted into the amount of released hydrogen at each temperature. Hydrogenation experiments were carried out in PCI mode only.

A Bruker D8 Advance X-ray powder diffractometer (CuKα radiation), equipped with secondary beam monochromator, was used for all diffraction measurements. All samples were always protected from air in a special holder covered with Kapton film; this was displaced from the diffraction plane, so as to avoid polymer contribution to the recorded pattern.

Infrared spectra were recorded by a JASCO FT/IR-4100A spectrophotometer in the 400 to 4000 cm^{-1} wavenumber range (2 cm^{-1} resolution). The powder sample was mixed with nujol and inserted between two KBr windows, sealed externally in glove box for air protection.

3. RESULTS AND DISCUSSION

3.1. Synthesis and properties of the Mg_2FeH_6 hydride. X-ray measurements on the ball milled $2MgH_2$+α-Fe powder showed the presence of Mg_2FeH_6 and alpha-iron only, without traces of either MgH_2 or Mg. Thus, all magnesium hydride was consumed in the $6MgH_2+3Fe \rightarrow 2Mg_2FeH_6+2Mg+Fe$ reaction; the residual Mg was not observed because it was possibly in nanocrystalline state. After the hydrogenation step in the Sievert apparatus, again the sole presence of Mg_2FeH_6 and of a variable quantity of α-Fe (clearly decreasing with synthesis time) could be detected in the X-ray data (Figure 1). The amount of iron dropped from the 3 to the 4 days run, and then decreased very slowly to a constant value after 9 days. Thus, the direct synthesis reaction $2Mg+Fe+3H_2 \rightarrow Mg_2FeH_6$ was not complete in the Sievert equipment, leaving a fraction of not reacted Fe in the sample; this agrees with what reported in previous work on the magnesium iron hydride system.[21] On the other hand, the small quantity of Mg left did not react directly with hydrogen to form magnesium hydride, but it cannot be detected in the X-ray pattern because presumably in nanocrystalline or non-crystalline form.

The relative Fe/Mg_2FeH_6 amount was determined by means of two-phase Rietveld refinements (FULLPROF computer package[24]). For 9-days synthesized Mg_2FeH_6, a weight composition of 5.8(1)% Fe and 94.2(1)% Mg_2FeH_6 was obtained, corresponding to a Fe/Mg_2FeH_6 weight ratio of 0.062. The refined cubic unit-cell parameters were a = 6.4435(3)

and 2.8611(2) Å for Mg_2FeH_6 (space group *Fm-3m*) and α-Fe (space group *Im-3m*), respectively. Final values of the agreement factors: R_p=0.127, wR_p=0.160, reduced χ^2=1.9.

A TPD run was performed on the Mg_2FeH_6 sample in the Sievert apparatus under 3 bar of hydrogen pressure. The inflexion point of the decomposition profile was located at 350 °C, and a total H_2 release of 4.8 wt% up to 550 °C was observed. This compares well with the expected value of 4.9%, obtained from the ideal H_2 yield of 5.47 wt% of pure Mg_2FeH_6 by correction for the iron and magnesium impurities content.

3.2. Steps of $2LiBH_4/Mg_2FeH_6$ dehydrogenation. The 2:1 nominal molar ratio was selected for the $LiBH_4/Mg_2FeH_6$ system, in order to study all multiple dehydrogenation steps of $LiBH_4$ reacting with subsequent products of previous reactions. The theoretical hydrogen yield of Mg_2FeH_6-$2LiBH_4$ is 7.85 wt%, considering that not decomposed LiH should be present in the final product. This can be an attractive value for many applications, in case it is coupled to a decreased dehydrogenation temperature with respect to that of pure $LiBH_4$.

Isothermal (PCI) H_2 desorption experiments were performed at eight temperatures in the 325-550 °C range. In four of these cases, hydrogen absorption was carried out as well. The results of full desorption and absorption cycles for two isotherms are shown in Figure 2. We discuss hereafter desorption results; for absorption, cf. the next section. Three pressure plateaus can be observed in all desorption experiments, indicating distinct dehydrogenation reactions which are denoted as A, B, and C in the decreasing pressure order. The A process was not observed in the isotherms at T > 400 °C, because the maximum applied pressure of about 100 bar was not sufficient to prevent the reaction from occurring already during the heating step. The A dehydrogenation reaction is the most demanding one kinetically: over 2 h waiting time was necessary for the equilibration at each pressure step, whereas about 0.5 and 1.5 h was sufficient on the average for the B and C processes, respectively.

In order to understand the dehydrogenation chemistry of the three processes, the isothermal experiments at 345 and 375 °C were repeated in the following way. Hydrogen desorption was interrupted after the A and B reactions, the sample holder was quenched in water, and X-ray powder patterns were recorded. X-ray data were collected at the beginning (before A) and at the end (after C) of desorption, too. In another experiment at 345 °C FTIR spectra were collected on the samples obtained after A and B in desorption mode, and after the B+C reaction in absorption mode.

The X-ray results of the experiment at 375 °C are shown in Figure 3; those obtained at 345 °C are the same. In Figure 4 the FTIR spectra referring to the 345 °C experiment are reported. After reaction A, MgH_2, FeB and LiH are formed as products. This proves that $LiBH_4$ indeed reacts with Mg_2FeH_6 during this dehydrogenation process. A possible reaction of lithium borohydride with the residual iron present in the sample was investigated independently, by performing a PCI experiment on the $LiBH_4$+Fe assemblage at the same temperature. The decomposition isotherm was identical to that of pure $LiBH_4$, thus excluding any direct reaction with iron. Thus, the most probable reaction occurring during process A is as follows:

$$2Mg_2FeH_6 + 2LiBH_4 \rightarrow 2LiH + 4MgH_2 + 2FeB + 5H_2 \quad (1)$$

A small amount of residual Mg_2FeH_6 appears among the products, indicating that when the sample was taken out of the Sievert device (just at the end of the A horizontal plateau) the reaction was not fully completed yet.

The B process can be interpreted unambiguously as the dehydrogenation reaction of MgH_2, as the Bragg peaks of magnesium hydride disappear after B and are replaced by the those of Mg:

$$MgH_2 \rightarrow Mg + H_2 \quad (2)$$

No role should be played by $LiBH_4$ in this process, because MgB_2 is not formed.

In the final product of dehydrogenation, in addition to the previous H-free compounds also the new Bragg peaks of MgB_2 are observed. This proves that in the C step the residual amount of $LiBH_4$ has reacted with Mg according to:

$$2LiBH_4 + Mg \rightarrow 2LiH + MgB_2 + 3H_2 \quad (3)$$

A reaction of $LiBH_4$ with MgH_2 can be excluded, because magnesium hydride had disappeared after the B step.

At variance with the $LiBH_4$+MgH_2 system, the dehydrogenation thermodynamics of the $LiBH_4$+Mg assemblage is not reported as such in the literature. Only the catalytic effect of Mg on the lithium borohydride decomposition was studied.[25] However, reaction (3) was reported to occur[12] as the second part of the two-step dehydrogenation of $LiBH_4$+MgH_2, after decomposition of MgH_2 into Mg+H_2. Indeed, the second step was shown to follow route (3) at higher pressure when sufficient equilibration time is provided, whereas when pressure is reduced quickly to a lower value Mg would not be involved in the reaction, but the alternative route $2LiBH_4 + Mg \rightarrow 2LiH + Mg + 2B + 3H_2$ would be followed.[26] This is consistent with our result: reaction C occurs with slow pressure equilibration, so that Mg can react with $LiBH_4$ according to route (3).

Surprisingly, no peaks of $LiBH_4$ appear in the X-ray (a) and (b) patterns of Figure 3, although only half lithium borohydride was consumed in reaction A, and the rest of it must be involved in reaction C because of the observed H_2 release with formation of MgB_2 (cf. the (c) pattern). It should be noticed that $LiBH_4$ melts at 280 °C; as PCI experiments were carried out at a higher temperature, re-solidification of unreacted lithium borohydride in nanocrystalline or amorphous form may have occurred. Indeed, results of FTIR measurements show clearly the presence of $LiBH_4$ after the A and B reactions (spectrum (a) in Figure 4). The three IR absorption peaks at 2225, 2291 and 2380 cm^{-1} correspond to active B-H stretching modes, and the peak at 1125 cm^{-1} indicates a B-H bending.[27-29] Further, after re-

hydrogenation the fingerprints of $LiBH_4$ appear with even greater evidence (spectrum (b) in Figure 4), but the corresponding X-ray pattern shows only the peaks of MgH_2 and FeB. Our results are consistent with what reported by other authors, who found the X-ray peaks of $LiBH_4$ to be hardly visible after re-solidification from melt,[25] and who could detect by FTIR but not by X-ray measurements lithium borohydride formed by hydrogenation of the $2LiH+MgB_2$ assemblage.[30]

In summary, the global desorption reaction can be written as A+4B+C:

$$2Mg_2FeH_6+4LiBH_4 \rightarrow 4LiH+3Mg+2FeB+MgB_2+12H_2 \qquad (4)$$

corresponding to a theoretical hydrogen yield of 7.85 wt%. Taking into account that the actual molar ratio of $LiBH_4$ to Mg_2FeH_6 is slightly larger than the nominal value of 2, because of the presence of little residual iron and magnesium in the as-synthesized Mg_2FeH_6 sample, the small excess of $LiBH_4$ is presumed to have reacted with excess Mg in reaction C.

In a previous dehydrogenation study of the $5LiBH_4/Mg_2FeH_6$ mixture[31] no clear diffraction peaks could be detected in the X-ray pattern of the decomposed sample, possibly because of the small content of magnesium iron hydride and/or the absorption of the parafilm used. Therefore, the phases obtained could not be identified. The Differential Scanning Calorimeter (DSC) pattern in flowing N_2 showed two peaks at 367 and 410 °C, which were tentatively interpreted as due to decomposition of pure Mg_2FeH_6, and to dehydrogenation of $LiBH_4$ reacting with Fe and Mg, respectively. On the basis of our phase identifications, we suggest to relate such DSC peaks to the A and B processes considered above (cf. reactions (1) and (2)).

3.3. Reaction reversibility and thermodynamic properties. The final samples obtained after full decomposition (4) could always be rehydrogenated successfully in the Sievert apparatus. However, only the equivalent of the H_2 amount released in the C and B steps was reabsorbed, whereas the A reaction could not be reversed (Figure 2). In the absorption cycles

at lower temperatures, the C and B plateaus appear to be distinct; then the reversible B+C process can be clearly identified with the two-step reaction $2LiBH_4 + MgH_2 \leftrightarrow 2LiBH_4 + Mg + H_2 \leftrightarrow 2LiH + MgB_2 + 4H_2$ previously proposed for the $2LiBH_4 + MgH_2$ composite.[12] Above 350 °C the two absorption steps merge into a single one, according to the one-step $2LiH + MgB_2 + 4H_2 \rightarrow 2LiBH_4 + MgH_2$ hydrogenation reaction.[30] This reaction was found to occur also in rehydrogenation experiments carried out at 445 °C on products of the decomposition of the $5LiBH_4/Mg_2FeH_6$ mixture.[31]

Comparable amounts of exchanged H_2 are observed in absorption and desorption modes for both the B and C steps. Re-desorption experiments were also performed after absorption, showing a very good reproduction of the B and C dehydrogenation steps as in the first desorption cycle.

The *p(T)* equilibrium relationships (desorption mode) were determined for each of the three A, B, and C reactions, by measuring the pressure values at inflexion points of all isothermal plateaus. On this basis, the corresponding van't Hoff plots $\ln(p/p_0) = \Delta_r S/R - (\Delta_r H/R)(1/T)$ were obtained, and they are shown in Figure 5. The corresponding $\Delta_r H$ and $\Delta_r S$ values, fitted by linear regression and normalized to 1 mole of H_2, are reported in Table 1. Also the plots for decomposition of the pure $LiBH_4$, Mg_2FeH_6 and MgH_2 hydrides from the literature[9,16,32] are shown in Figure 5 for the sake of comparison; in Table 2 the corresponding reaction enthalpies and entropies are given. For Mg_2FeH_6, the entropy for data from Ref. 16 was derived by the van't Hoff fitting of original points; results by other authors[18-20] are also reported for comparison.

By inspection of Figure 5, the van't Hoff plot of process A lies well above the decomposition lines of Mg_2FeH_6 and $LiBH_4$ (and also of MgH_2). This proves definitely that both components of the composite are strongly destabilized thermodynamically by reacting together with formation of iron boride FeB, according to reaction (1). For the sake of

comparison it can be useful to extrapolate the ideal dehydrogenation temperature at standard pressure by the $\Delta_r H/\Delta_r S$ approximation, on neglecting the thermal dependence of enthalpy and entropy. We get 217 °C, to be compared with 302-319 °C for Mg_2FeH_6 and 370 °C for $LiBH_4$, on the basis of data in Table 2. Thus, the first H_2 desorption step of the $2LiBH_4$-Mg_2FeH_6 composite is confirmed to be thermally more favourable than dehydrogenation of either pure hydride component. Interestingly, this result is due not to the reaction enthalpy, which is comparable for the three reactions (cf. Tables 1 and 2, and the slopes of van't Hoff plots in Figure 5), but to the entropy, which is substantially larger for reaction (1) than for decomposition of either simple hydride. Therefore in this case the thermodynamic destabilization (i.e., the decrease of $\Delta_r G = \Delta_r H - T\Delta_r S$) is due to the entropic rather than to the enthalpic effect.

According to plots of Figure 5, reaction B is clearly confirmed to be the dehydrogenation of magnesium hydride; the numerical values of van't Hoff parameters in Table 1 match well with literature data (Table 2). Reaction C shows a remarkably smaller enthalpy than all other processes (including those of Table 2). This enthalpy is comparable to that given in the literature for decomposition of the $LiBH_4$+MgH_2 assemblage in a single step;[10] we are not aware of previous results for the individual second step C. Indeed, it is interesting to notice how the plots of reactions B and C are well separated in Figure 5, fully consistent with the two-step model proposed for the $LiBH_4$+MgH_2 decomposition.[12] Thus, $LiBH_4$ is destabilized by reaction (3) because of its smaller enthalpy, which overcompensates the slight increase of entropy, with respect to dehydrogenation of pure $LiBH_4$ (cf. also Figure 5).

The results of TPD measurements are shown in Figure 6. Three curves were recorded at 3, 20 and 80 bar of hydrogen pressure. In the 3 bar data the A and B processes are not resolved but merged in a single inflexion point at 345 °C. At higher pressures, on the other hand, the inflexion point splits clearly into two ones corresponding to A and B reactions (380 and 401

°C at 20 bar, 414 and 472 °C at 80 bar). The C reaction appears only in the 3 bar experiment (at 460 °C), whereas it moves above the upper *T* limit of the experimental setup (550 °C) in the high pressure runs. On comparing the TPD pairs of *p*,*T* values for each reaction with the corresponding PCI results (cf. the van't Hoff plot of Figure 5), lower *p*/higher *T* values are observed as expected, due to the large hysteresis effects of the dynamic thermal ramp mode even with low heating rate. The qualitative agreement is however good, confirming the sequence of reactions determined by the more accurate isothermal mode.

The scheme of dehydrogenation reactions should be discussed also in connection with the amount of hydrogen released in the three different identified steps. In Table 3, the average values of desorbed H_2 wt% (PCI and TPD results) are given for the A, B, C processes and for the overall decomposition reaction. Significant deviations from the PCI averages can be observed for individual isotherms (cf. also Figure 2). For comparison, the theoretical ideal wt% values are reported, too; these quantities are always referred to the initial weight of the $2LiBH_4$-Mg_2FeH_6 composite. As a small fraction of unreacted Fe and Mg is present in the sample, as discussed in the previous section, the ideal overall H_2 wt% should be corrected accordingly. On using the Fe/Mg_2FeH_6 weight ratio obtained by Rietveld refinement of the X-ray pattern, an expected overall wt% hydrogen yield of 7.45% is obtained for the system (cf. the ideal value of 7.85%). The other corrected values for individual reaction steps are also reported in the last column of Table 3. Average PCI and TPD results are slightly lower than expected for the B and C reactions; the deficit is somehow larger for the A step (from PCI rather than TPD data). On the whole, therefore, the observed relative amounts of desorbed hydrogen are consistent with the interpretation of reactions A, B and C according to (1), (2), and (3).

4. CONCLUSIONS

The $2LiBH_4$-Mg_2FeH_6 composite has proved to undergo dehydrogenation in three distinct steps A, B, and C. Reaction A occurs well within the *p(T)* stability regions of both pure components, with formation of the mixed compound FeB. Each of the two hydrides is found to be really destabilized thermodynamically by the presence of the other one in desorption conditions; the effect was shown to be of entropic rather than enthalpic nature. As an example, at 30 bar of H_2 pressure the composite should decompose at 330 °C, whereas at the same pressure Mg_2FeH_6 would release H_2 only at 455 °C, and $LiBH_4$ even at 580 °C. For comparison, also MgH_2 would require heating to 425 °C to decompose at 30 bar. This confirms that the destabilization method[6] may be quite effective in a broad chemical context. Of course, however, the wt% hydrogen yield of the composite from reaction A is smaller than the full decomposition yields of the two single hydrides. Further, below $p(H_2)$ = 100 bar the reaction A could not be reversed, so that higher pressures would be possibly necessary to re-hydrogenate FeB.

The B and C steps are well reversible, and they correspond to two distinct decomposition stages of the well known $LiBH_4$-MgH_2 assemblage, according to what previously found by different experimental methods.[12] In particular, the present study provides a full thermodynamic characterization of the poorly defined second stage C (reaction of $LiBH_4$ with Mg). We thus believe that fruitful results will be obtained in the future by extending investigations on the dehydrogenation properties of complex hydride systems.

AUTHOR INFORMATION

Corresponding Author

*E-mail: catti@mater.unimib.it

REFERENCES

(1) Jepse, J.; Bellosta von Colbe, JM.; Klassen, T.; Dornheim, M. *Int. J. Hydrogen Energy* **2012**, *37*, 4204-4214.

(2) David, W.I.F. *Faraday Discuss.* **2011**, *151*, 399-414.

(3) Song, L.; Wang, S.; Jiao, C.; Si, X.; Li, Z.; Liu, S.; Liu, S.; Jiang, C.; Li, F.; Zhang, J.; Sun, L.; Xu, F.; Huang, F. *J. Chem. Thermodynamics* **2012**, *46*, 86-93.

(4) Fichtner, M. *Adv. Engin. Mater.* **2005**, *7*, 443-455.

(5) Züttel, A.; Borgschulte, A.; Orimo, S. *Scripta Mater.* **2007**, *56*, 823-828.

(6) Vajo, J.J.; Olson, G.L. *Scripta Mater.* **2007**, *56*, 829-34.

(7) Siegel, D.J.; Wolverton, C.; Ozolins, V. *Phys. Rev. B* **2007**, *76*, 134102/1-5.

(8) Züttel A.; Rentsch, S.; Fischer, P.; Wenger, P.; Sudan, P.; Mauron, Ph.; Emmenegger, Ch. *J. Alloys Compd.* **2003**, *356-357*, 515-520.

(9) Mauron, Ph.; Buchter, F.; Friedrichs, O.; Remhof, A.; Bielmann, M.; Zwicky, C.N.; Züttel, A. *J. Phys. Chem. B* **2008**, *112*, 906-10.

(10) Vajo, J.J.; Skeith, S.L.; Mertens, F. *J. Phys. Chem. B* **2005**, *109*, 3719-22.

(11) Pinkerton, F.E.; Meyer, M.S.; Meisner, G.P.; Balogh, M.P.; Vajo, J.J. *J. Phys. Chem. C* **2007**, *111*, 12881-85.

(12) Bösenberg U.; Doppiu S.; Mosegaard L.; Berkhordarian G.; Eigen N.; Borgschulte A.; Jensen T.R.; Cerenius Y.; Gutfleisch O.; Klassen T.; Dornheim M.; Bormann R. *Acta Mater.* **2007**, *55*, 3951-58.

(13) Zhang, Y.; Tian, Q.; Chu, H.; Zhang, J.; Sun, L.; Sun, J.; Wen, Z. *J. Phys. Chem. C* **2009**, *113*, 21964-69.

(14) Bardají EG, Zhao-Karger Z, Boucharat N, Nale A, van Setten MJ, Lohstroh W, Röhm E, Catti M, Fichtner M. *J. Phys. Chem. C* **2011**, *115*, 6095-101.

(15) Nale, A.; Catti, M.; Bardají, E.G.; Fichtner, M. *Int. J. Hydrogen Energy* **2011**, *36*, 13676-13682.

(16) Bogdanovic, B.; Reiser, A.; Schlichte, K.; Spliethoff, B.; Tesche, B. *J. Alloys Compd.* **2002**, *345*, 77-89.

(17) Sai Raman, S.S.; Davidson, D.J.; Bobet, J.-L.; Srivastava, O.N. *J. Alloys Compd.* **2002**, *333*, 282-290.

(18) Puszkiel, J.A.; Arneodo Larochette, P.; Gennari, F.C. *Int. J. Hydrogen Energy* **2008**, *33*, 3555-3560.

(19) Puszkiel, J.A.; Arneodo Larochette, P.; Gennari, F.C. *J. Alloys Compd.* **2008**, *463*, 134-142.

(20) Zhang, X.; Yiang, R.; Qu, J.; Zhao, W.; Xie, L.; Tian, W.; Li, X. *Nanotechnology* **2010**, *21*, 095706/1-7.

(21) Polanski, M.; Plocinski, T.; Kunce, I.; Bystrzycki, J. *Int. J. Hydrogen Energy* **2010**, *35*, 1257-1266.

(22) Wang, Y.; Cheng, F.; Li, C.; Tao, Z.; Chen, J. *J. Alloys Compd.* **2010**, *508*, 554-558.

(23) Polanski, M.; Nielsen, T.K.; Cerenius, Y.; Bystrzycki, J.; Jensen, T.R. *Int. J. Hydrogen Energy* **2010**, *35*, 3578-3582.

(24) Rodriguez-Carvajal, J. FULLPROF: a program for Rietveld refinement and pattern matching analysis. /http://www.ill.eu/sites/fullprof/S.

(25) Orimo, S.; Nakamori, Y.; Kitahara, G.; Miwa, K.; Ohba, N.; Towata, S.; Zuttel, A. *J. Alloys Compd.* **2005**, *404-406*, 427-430.

(26) Kou, H.; Xiao, X.; Chen, L.; Li, S.; Wang, Q. *Trans. Nonferrous Met. Soc. China* **2011**, *21*, 1040-1046.

(27) Harvey, K.B.; McQaker, N.R. *Canad. J. Chem.* **1971**, *49*, 3282-3286.

(28) Gomes, S.; Hagemann, H.; Yvon, K. *J. Alloys Compd.* **2002**, *346*, 206-210.

(29) Brampton, D. *Destabilization of lithium borohydride with additions of magnesium hydride*. MRes. Thesis **2008**, University of Birmingham.

(30) Shaw, L.L.; Wan, X.; Hu, J.Z.; Kwak, J.H.; Yang, Z. *J. Phys. Chem. C* **2010**, *114*, 8089-8098.

(31) Langmi, H.W.; McGrady, G.S.; Newhouse, R.; Rönnebro, E. *Int. J. Hydrogen Energy* **2012**, *37*, 6694-6699.

(32) Bogdanovic, B.; Bohmhammel, K.; Christ, B.; Reiser, A.; Schlichte, K.; Vehelen, R.; Wolf, U. *J. Alloys Compd.* **1999**, *282*, 84-92.

Table 1 – Thermodynamic parameters (PCI measurements, Figure 5) for the H_2 desorption steps of the $2LiBH_4$-Mg_2FeH_6 composite, referred to 1 mole of H_2. The e.s.d.'s are given in parentheses.

	Chemical reaction	$\Delta_r H$ (kJ mol^{-1})	$\Delta_r S$ (J K^{-1} mol^{-1})	T range (°C)
A	$2Mg_2FeH_6 + 2LiBH_4 \rightarrow 2LiH + 4MgH_2 + 2FeB + 5H_2$	72(4)	147(7)	310-400
B	$MgH_2 \rightarrow Mg + H_2$	74.6(7)	138.0(8)	310-440
C	$2LiBH_4 + Mg \rightarrow 2LiH + MgB_2 + 3H_2$	48(2)	87(2)	350-530

Table 2 – Literature thermodynamic parameters for the dehydrogenation reactions of Mg_2FeH_6, MgH_2 and $LiBH_4$, referred to 1 mole of H_2.

Chemical reaction	$\Delta_r H$ (kJ mol^{-1})	$\Delta_r S$ (J K^{-1} mol^{-1})	Ref.
$2Mg_2FeH_6 \rightarrow 2Mg + Fe + 3H_2$	77	134	16
	87(3)	147(15)	18
	80(7)	137(13)	19
	79	135	20
$MgH_2 \rightarrow Mg + H_2$	74.5	135	32
$2LiBH_4 \rightarrow 2LiH + 3H_2$	74	115	9

Table 3 - Average hydrogen yields of the decomposition steps of the $2LiBH_4$- Mg_2FeH_6 composite from isothermal (PCI) and dynamic (TPD) measurements, compared with ideal and corrected values (cf. the text).

	PCI H wt%	TPD H wt%	ideal H wt%	corrected H wt%
A	1.9	2.6	3.27	2.93
B	2.2	2.0	2.62	2.34
C	2.0	1.9	1.96	2.18
Total	6.1	6.5	7.85	7.45

Captions of the figures.

Figure 1. X-ray diffraction pattern (CuKα radiation) of the as-synthesized Mg_2FeH_6 hydride.

Figure 2. PCI (Pressure-Composition-Isotherm) results on the $2LiBH_4$-Mg_2FeH_6 system for the 345 and 375 °C isotherms. Open and full symbols indicate H_2 desorption and absorption processes, respectively. A, B and C denote pressure plateaus corresponding to three distinct desorption steps.

Figure 3. X-ray diffraction patterns (CuKα radiation) of the subsequent products of dehydrogenation of the $2LiBH_4$-Mg_2FeH_6 composite after reactions A (a) and B (b), and the final product after reaction C (c), as obtained by PCI experiment at 375 °C.

Figure 4. FTIR spectra (a) of H_2 desorption products of $2LiBH_4$-Mg_2FeH_6 after reaction B, and (b) of H_2 absorption products after reactions C+B (cf. Fig. 2).

Figure 5. Van't Hoff plots of the three dehydrogenation steps A, B, C of the $2LiBH_4$-Mg_2FeH_6 composite from PCI desorption results (full symbols including best fit lines). Open symbols denote literature data for the $LiBH_4$ (circles),[9] and Mg_2FeH_6 (squares)[16] decompositions. The dotted line without symbols corresponds to MgH_2 dehydrogenation.[32]

Figure 6. Dynamic thermal decomposition of $2LiBH_4$-Mg_2FeH_6 under variable hydrogen pressure (heating rate 1 °C min^{-1} in Sievert apparatus). Inflexion points denoting the subsequent steps of the reaction are indicated by corresponding symbols.

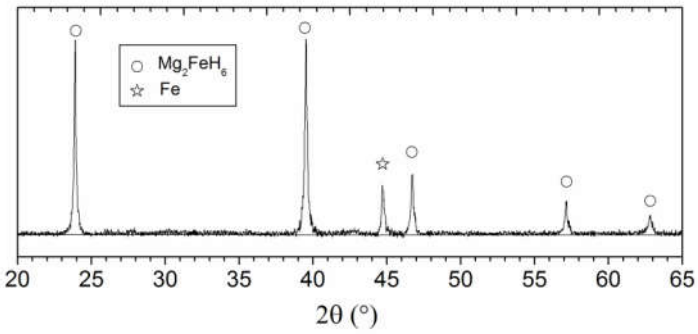

Figure 1

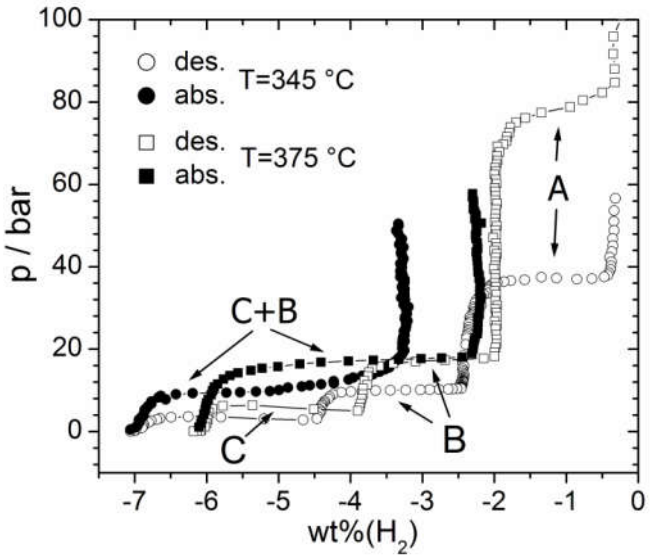
des.
abs.
T=345 °C
des.
abs.
T=375 °C
A
C+B
C
B
p / bar
wt%(H2)
100
80
60
40
20
0
-7
-6
-5
-4
-3
-2
-1
0

Figure 2

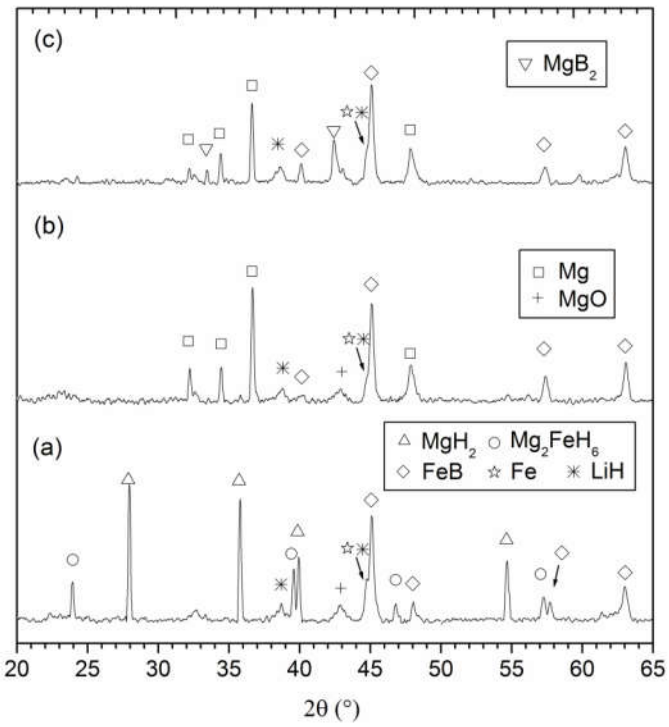
(c)
MgB2
(b)
Mg
MgO
(a)
MgH2
Mg2FeH6
FeB
Fe
LiH
20
25
30
35
40
45
50
55
60
65
2θ (°)

Figure 3

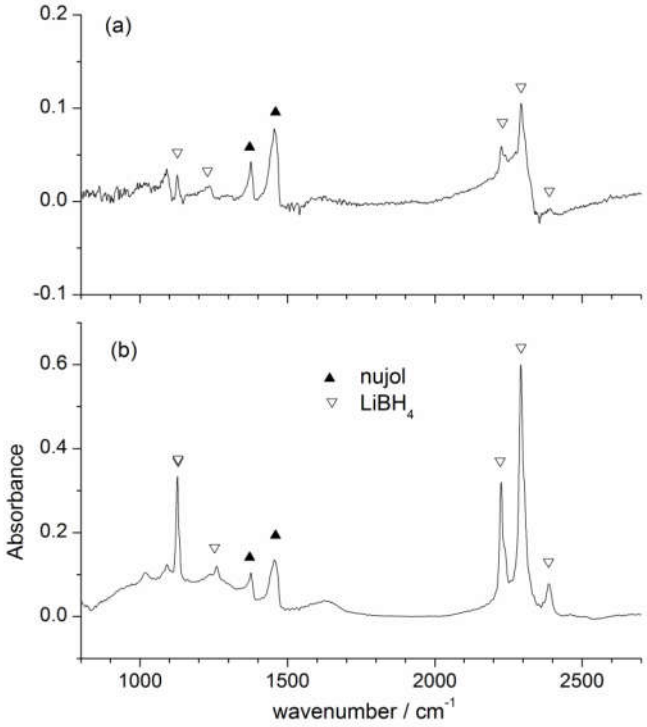
(a)
(b)
nujol
LiBH4
Absorbance
wavenumber / cm-1
0.2
0.1
0.0
-0.1
0.6
0.4
0.2
0.0
1000
1500
2000
2500

Figure 4

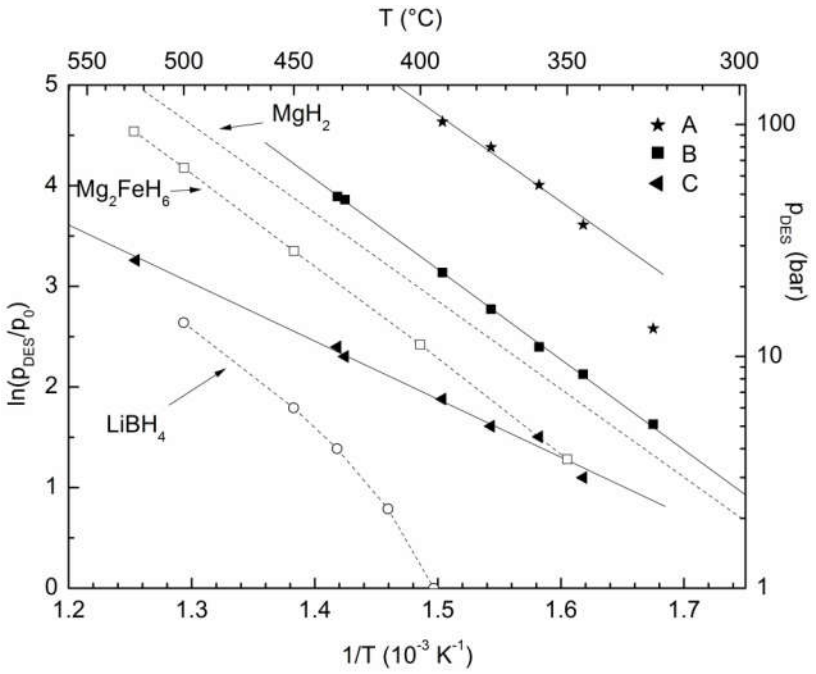
T (°C)
550
500
450
400
350
300
5
4
3
2
1
0
MgH2
Mg2FeH6
LiBH4
A
B
C
100
10
1
pDES (bar)
ln(pDES/p0)
1.2
1.3
1.4
1.5
1.6
1.7
1/T (10-3 K-1)

Figure 5

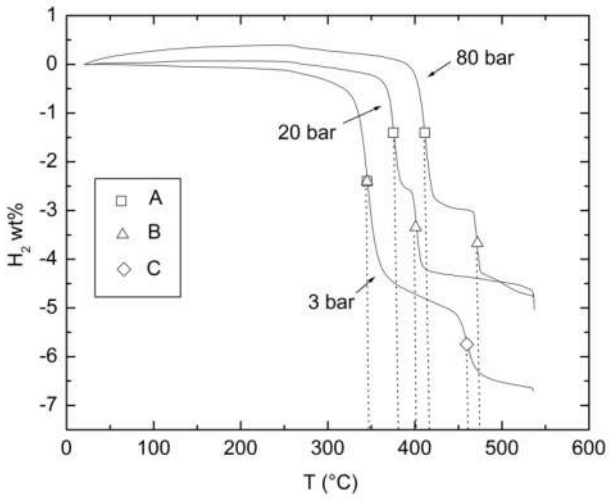
80 bar
20 bar
3 bar
A
B
C
H2 wt%
T (°C)
1
0
-1
-2
-3
-4
-5
-6
-7
0
100
200
300
400
500
600

Figure 6

TABLE OF CONTENTS IMAGE